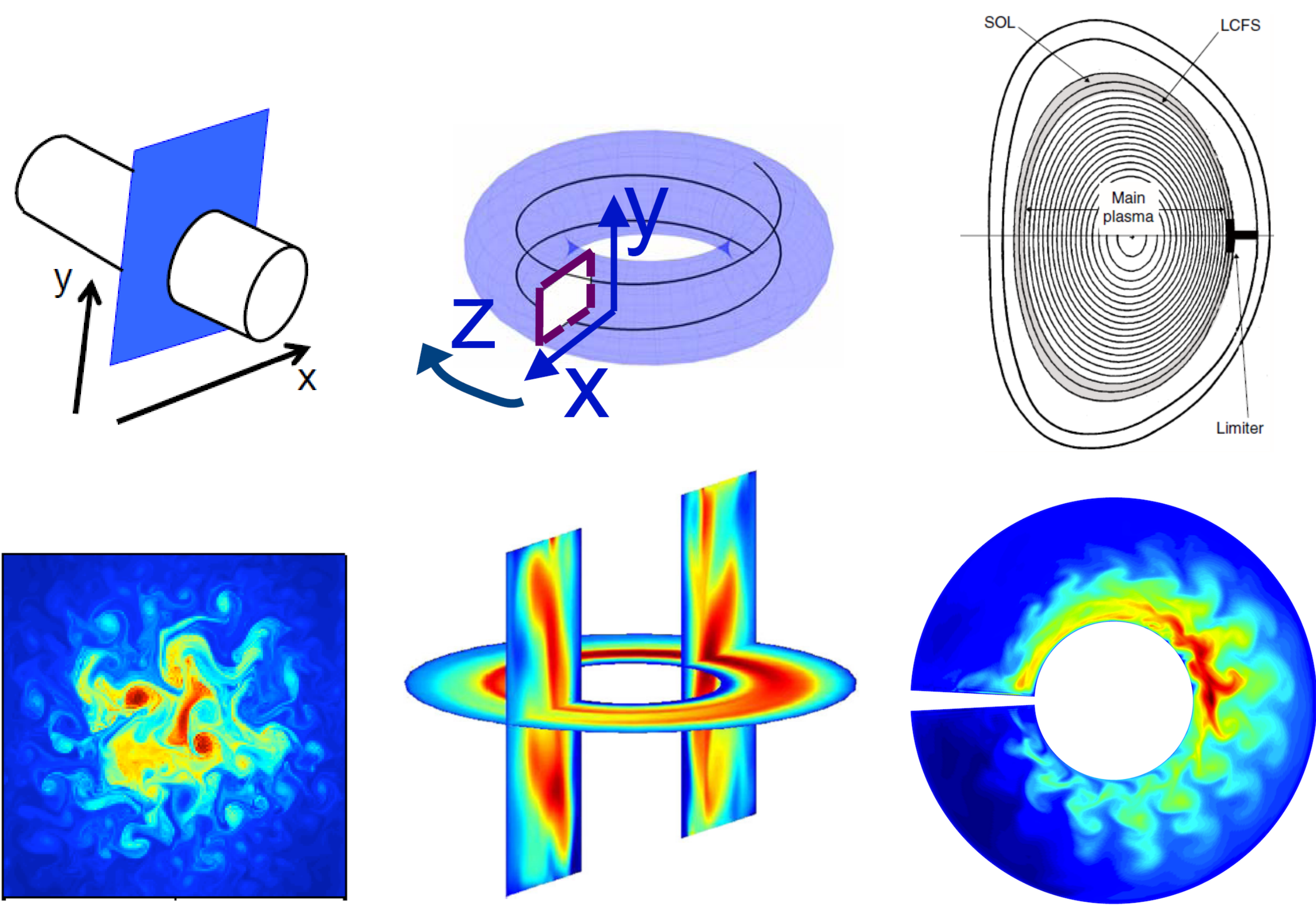


1. Motivation



$$\frac{\partial n}{\partial t} = R[\phi, n] + 2 \left(n \frac{\partial T_e}{\partial y} + T_e \frac{\partial n}{\partial y} - n \frac{\partial \phi}{\partial y} \right) + D_n \nabla_{\perp}^2 n - n \frac{\partial V_{\parallel e}}{\partial z} - V_{\parallel e} \frac{\partial n}{\partial z} + S_n, \quad (1)$$

$$\frac{\partial \nabla_{\perp}^2 \phi}{\partial t} = R[\phi, \nabla_{\perp}^2 \phi] - V_{\parallel i} \frac{\partial \nabla_{\perp}^2 \phi}{\partial z} + 2 \left(\frac{T_e}{n} \frac{\partial n}{\partial y} + \frac{\partial T_e}{\partial y} \right) + \frac{1}{n} \frac{\partial j_{\parallel}}{\partial z} - \frac{\eta_0}{n} \left(2 \frac{\partial^2 V_{\parallel i}}{\partial y \partial z} + \frac{\partial^2 \phi}{\partial y^2} \right) + D_{\phi} \nabla_{\perp}^4 \phi, \quad (2)$$

$$\frac{\partial T_e}{\partial t} = R[\phi, T_e] - V_{\parallel e} \frac{\partial T_e}{\partial z} + \frac{4}{3} \left(T_e \frac{\partial T_e}{\partial y} - T_e \frac{\partial \phi}{\partial y} \right) + D_T \nabla_{\perp}^2 T_e + \frac{2}{3} \frac{T_e}{n} \frac{\partial j_{\parallel}}{\partial z} - \frac{2}{3} T_e \frac{\partial V_{\parallel e}}{\partial z} + S_T, \quad (3)$$

$$\frac{m_e}{m_i} \frac{\partial V_{\parallel e}}{\partial t} = \frac{m_e}{m_i} n R[\phi, V_{\parallel e}] - \frac{m_e}{m_i} n V_{\parallel e} \frac{\partial V_{\parallel e}}{\partial z} - T_e \frac{\partial n}{\partial z} + n \frac{\partial \phi}{\partial z} - 1.71 n \frac{\partial T_e}{\partial z} + n v_{j_{\parallel}} + \frac{4}{3} \frac{\eta_0}{n} \frac{\partial^2 V_{\parallel e}}{\partial z^2} + \frac{2}{3} \frac{\eta_0}{n} \frac{\partial^2 \phi}{\partial y \partial z} - \frac{2}{3} \frac{\eta_0}{n} \frac{\partial^2 p_e}{\partial z \partial y} + D_V \nabla_{\perp}^2 V_{\parallel e}, \quad (4)$$

$$n \frac{\partial V_{\parallel i}}{\partial t} = n R[\phi, V_{\parallel i}] - n V_{\parallel i} \frac{\partial V_{\parallel i}}{\partial z} - T_e \frac{\partial n}{\partial z} - n \frac{\partial T_e}{\partial z} + \frac{4}{3} \frac{\eta_0}{n} \frac{\partial^2 V_{\parallel i}}{\partial z^2} + \frac{2}{3} \frac{\eta_0}{n} \frac{\partial^2 \phi}{\partial y \partial z} + D_V \nabla_{\perp}^2 V_{\parallel i}, \quad (5)$$

► In fluid codes simulating the edge of magnetically confined plasmas, boundary conditions at the target plates are imposed at the magnetic presheath entrance (MPSE).

► For example a global 3D fluid code based on the electrostatic drift-reduced Braginskii equations, the Global Braginskii Solver (GBS) [1,2], has been used to simulate the TORPEX device [3] and other basic plasma physics experiments.

► **The boundary conditions strongly affect several properties of the plasma**, imposing the plasma losses at the wall and therefore the steady state profiles and the plasma circulation.

2. The drift-reduced approximation

The drift-reduced approximation (DRA) assumes that the ions perpendicular dynamics is dominated by the $\mathbf{E} \times \mathbf{B}$ and diamagnetic drifts, and the polarization drift is computed to zeroth order,

$$\mathbf{v}_{\perp i}^{\text{dra}} = \mathbf{V}_{\mathbf{E} \times \mathbf{B}} + \mathbf{V}_{\text{di}} + \mathbf{V}_{\text{pol}}^0 \quad \text{with} \quad \mathbf{V}_{\text{pol}}^0 = \frac{\mathbf{b}}{\omega_{ci}} \times [((\mathbf{V}_{\mathbf{E} \times \mathbf{B}} + V_{\parallel i} \mathbf{b}) \cdot \nabla) \mathbf{V}_{\mathbf{E} \times \mathbf{B}}] \ll \mathbf{V}_{\mathbf{E} \times \mathbf{B}} \quad (1)$$

At the MPSE equation (1) is not valid anymore and so the DRA breaks down.

3. The magnetic presheath entrance location

At the MPSE ions inertia becomes important compared to the magnetic force and they get deflected by the electric field. Instead, electrons remain magnetized almost all the way up to the wall.

The location of the MPSE is derived using the method recently described in [4]. In the limit $T_i \ll T_e$ and $\nabla = \partial_N$, the presheath condition $n_i = n_e$ and $V_{ix} = V_{\mathbf{E} \times \mathbf{B}}$ leads to a matrix system $\mathbf{M} \vec{X} = \vec{S}$, where

$$\mathbf{M} = \begin{pmatrix} V_{iN} n \sin \alpha & 0 \\ 0 & V_{iN} \\ -T_e & 0 \end{pmatrix}, \quad \vec{X} = \begin{pmatrix} \partial_N n \\ \partial_N V_{\parallel i} \\ \partial_N \phi \end{pmatrix}, \quad \vec{S} = \begin{pmatrix} S_{pi} \\ S_{mi} \\ S_{me} \end{pmatrix}.$$

In the presheath, gradients are small and due to the presence of sources. At the MPSE, non-zero gradients can be sustained without sources and $V_{ix} = V_{\mathbf{E} \times \mathbf{B}}$ is still valid.

This leads to $\mathbf{M} \vec{X} \simeq 0$ at the MPSE, and $\vec{X} \neq 0$ imposes $\det(\mathbf{M}) = 0$, giving

$$V_{iN} = c_s \sin \alpha \quad (2)$$

4. Boundary conditions

Boundary conditions at the MPSE:

$$V_{\parallel i} = (1 - \delta) c_s - V_{E_x} / \tan \alpha \quad (3)$$

$$V_{\parallel e} = c_s \exp(\Lambda_m - e\phi / T_e) - V_{E_x} / \tan \alpha \quad (4)$$

$$\partial_N n = -(n / c_s) \partial_N V_{\parallel i} \quad (5)$$

$$\partial_N \phi = -(m_i c_s / e) \partial_N V_{\parallel i} \quad (6)$$

$$\nabla_{\perp}^2 \phi = -(m_i \cos^2(\alpha) / e) [(\partial_N V_{\parallel i})^2 + c_{sb} \partial_N^2 V_{\parallel i}] \quad (7)$$

where $\delta = \partial_y V_{ix} / \omega_{ci}$, $V_{E_x} = -E_x / B$ is the drift velocity due to an external electric field E_x .

Some important consequences:

► **Parallel flows:** $j_{\parallel} \neq 0$ is expected at the MPSE.

► **Effect of $\mathbf{E} \times \mathbf{B}$:** $V_{\parallel i}$ can reverse sign at the MPSE if the $\mathbf{E} \times \mathbf{B}$ flow exceeds $c_s \tan \alpha$.

► **Global circulation:** $\nabla_{\perp}^2 \phi^{\text{edge}} < 0$, $\nabla_{\perp}^2 \phi^{\text{bulk}} / \nabla_{\perp}^2 \phi^{\text{edge}} \sim (\rho_s / L_{\perp})^2 \ll 1$ so imposes a global circulation.

5. Numerical verification

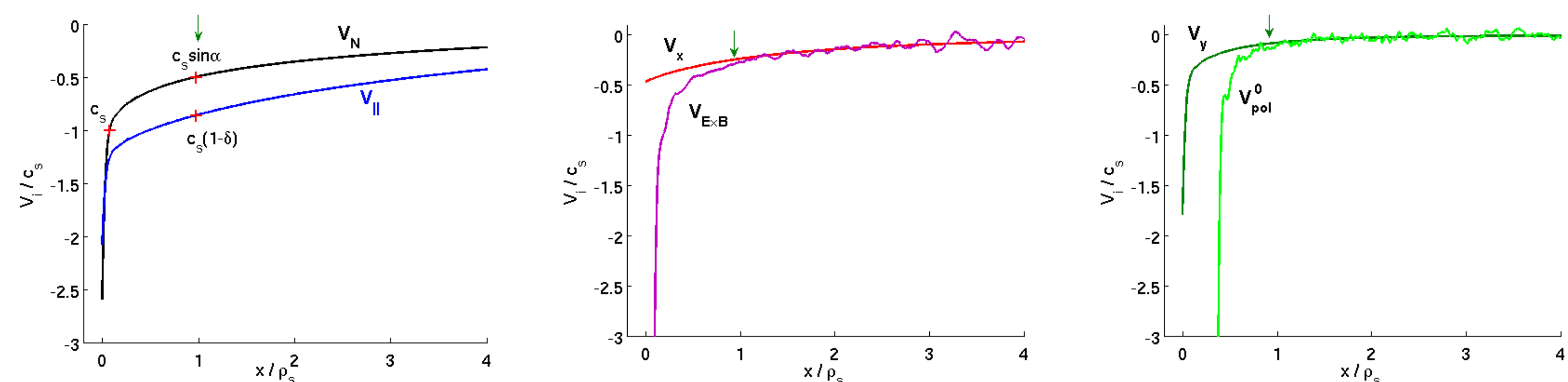
Numerical simulations were performed with ODISEE (One-Dimensional Sheath Edge Explorer) [4], a 1d3v PIC code solving the Vlasov-Poisson system for a plasma between two absorbing walls.

► $T_i \ll T_e$

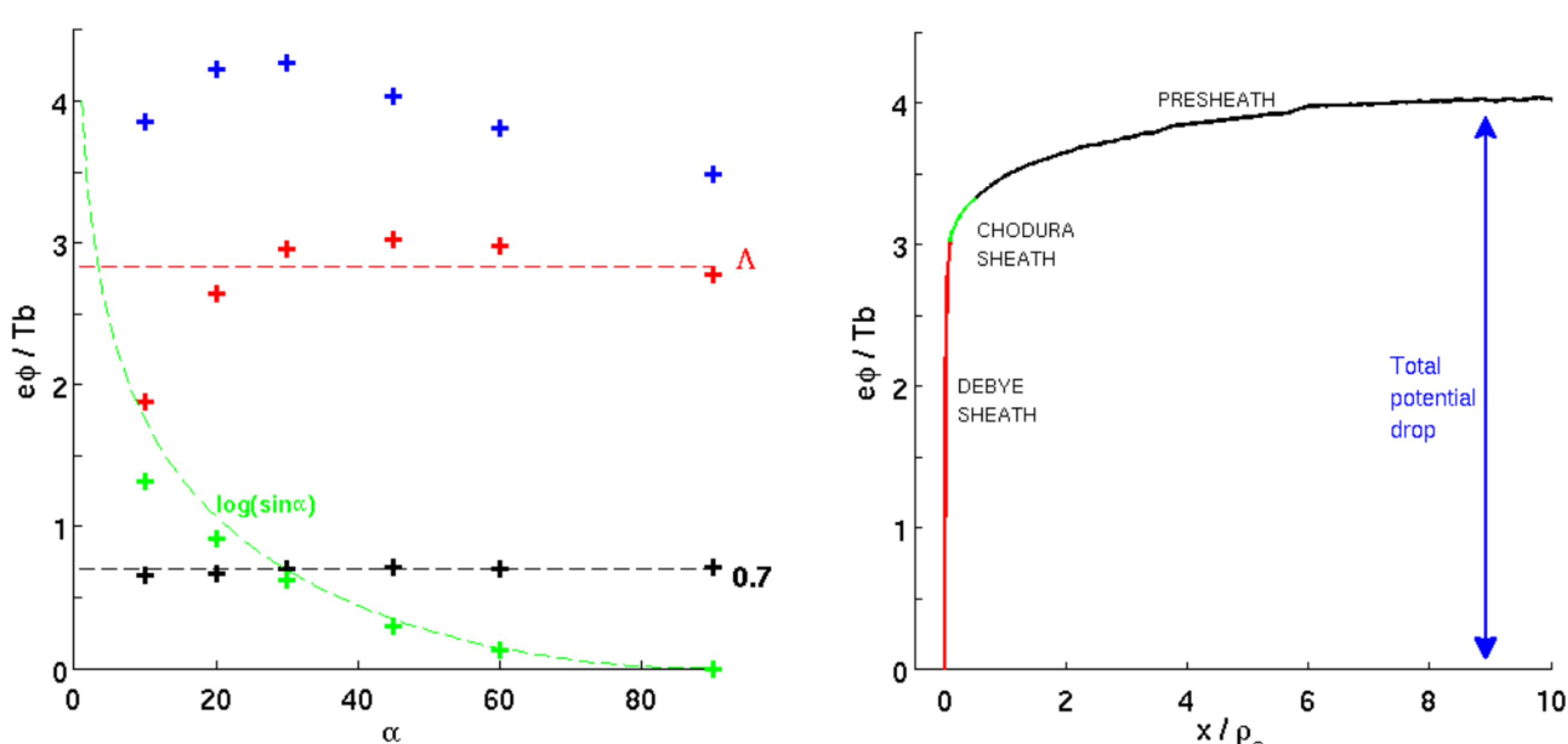
► $L_{\text{system}} \sim 20 \rho_s$, $\rho_s \gg \lambda_D$, $\rho_e \sim \lambda_D$

► $S_p(x, \mathbf{v}) = S_0 f_{\text{max}}(\mathbf{v})$

► Ion velocity profiles for $\alpha = 30^\circ$:



► Potential drop as a function of α :



Thus $\Lambda_m = \Lambda - \log(\sin \alpha)$ for $\alpha > 30^\circ$, where $\Lambda = \log \sqrt{m_i / 2\pi m_e}$. For small angles, $\Lambda_m \approx \Lambda$.

6. Effects of perpendicular gradients

► Normal gradients ∂_N are in the ρ_s scale and perpendicular gradients along x are in a scale $L > \rho_s$.

► The gradient operator is written as $\partial_x \sim \sigma / L$ where $\sigma = \pm 1$ is the sign of the gradient.

► Only terms of order $\epsilon = \rho_s / L$ are kept.

This leads to a modified matrix,

$$\mathbf{M} = \begin{pmatrix} V_{iN} & n \sin \alpha & \frac{n}{B} \left([(1 - \delta) \cos \alpha - 1] \frac{\sigma_\phi}{L_\phi} - \frac{\sigma_n}{L_n} + \cos \alpha \frac{\partial_x V_{iy}}{V_{iN}} \right) \\ 0 & V_{iN} & (e / m_i) (\sin \alpha - \partial_x V_{iz} / \omega_{ci}) \\ -T_e & 0 & en \end{pmatrix}$$

and the solution of $\det(\mathbf{M}) = 0$ gives

$$V_{iN} = c_s \sin \alpha \sqrt{1 + \eta^2 - \eta} \quad (8)$$

where

$$\eta = \frac{1}{2} [(\cos \alpha (1 - \delta) - 1) \sigma_\phi \epsilon_\phi + \sigma_v \epsilon_v - \sigma_n \epsilon_n] / \sin \alpha \quad (9)$$

and

$$\epsilon_x = \frac{\rho_s}{L_x} \quad (10)$$

► The effect of perpendicular gradients on the MPSE is therefore smaller than previously predicted [5], this is because here we treat self-consistently the presence of $\mathbf{E} \times \mathbf{B}$ gradients through Faraday's law.

► The effect may become significant if the density and velocity gradients are not in phase.

7. Further work

References :

- [1] P. Ricci and B. N. Rogers, Turbulence phase space in Simple Magnetized Toroidal Plasmas, Phys. Rev. Lett. 104, 145001 (2010)
- [2] B. N. Rogers and P. Ricci, Low frequency turbulence in a linear magnetized plasma, Phys. Rev. Lett. 104, 225002 (2010)
- [3] A. Fasoli et al, Electrostatic Turbulence and Transport in a Simple Magnetized Plasma, Phys. Plasmas, 13, 055902, (2006)
- [4] J. Loizu, P. Ricci and C. Theiler, Existence of subsonic plasma sheaths, Physical Review E, 83, 016406 (2011)
- [5] S. Kuhn et al, The magnetized plasma-wall transition and its relation to fluid boundary conditions, Comput. Phys. Commun., 177 (2007)

The boundary conditions given by equations (4)-(8) will be implemented in the GBS code. The effect on steady-state profiles, fluctuation levels and plasma circulation will be studied.